Dual stratified mixed convection flow of Eyring-Powell fluid over an inclined stretching cylinder with heat generation/ absorption effect

Cite as: AIP Advances **6**, 075112 (2016); https://doi.org/10.1063/1.4959587
Submitted: 21 March 2016 • Accepted: 08 July 2016 • Published Online: 19 July 2016

Khalil Ur Rehman, M.Y. Malik, T. Salahuddin, et al.

AIP ADVANCES **6**, 075112 (2016)

Dual stratified mixed convection flow of Eyring-Powell fluid over an inclined stretching cylinder with heat generation/absorption effect

Khalil Ur Rehman, M.Y. Malik, T. Salahuddin,[a] and M. Naseer
Department of Mathematics, Quaid-i-Azam University, Islamabad 44000, Pakistan

(Received 21 March 2016; accepted 8 July 2016; published online 19 July 2016)

Present work is made to study the effects of double stratified medium on the mixed convection boundary layer flow of Eyring-Powell fluid induced by an inclined stretching cylinder. Flow analysis is conceded in the presence of heat generation/absorption. Temperature and concentration are supposed to be higher than ambient fluid across the surface of cylinder. The arising flow conducting system of partial differential equations is primarily transformed into coupled non-linear ordinary differential equations with the aid of suitable transformations. Numerical solutions of resulting intricate non-linear boundary value problem are computed successfully by utilizing fifth order Runge-Kutta algorithm with shooting technique. The effect logs of physical flow controlling parameters on velocity, temperature and concentration profiles are examined graphically. Further, numerical findings are obtained for two distinct cases namely, zero (plate) and non-zero (cylinder) values of curvature parameter and the behaviour are presented through graphs for skin-friction coefficient, Nusselt number and Sherwood number. The current analysis is validated by developing comparison with previously published work, which sets a benchmark of quality of numerical approach. [http://dx.doi.org/10.1063/1.4959587]

I. INTRODUCTION

An analysis of stratification phenomena in non-Newtonian fluids received substantial attention due to its practical applications in engineering and industrial areas. Stratification of medium appears due to temperature differences, variation of concentration or mixture of different fluids of distinct densities. For example geophysical flows, heat rejection into the environment such as seas, lakes and rivers, storage systems for thermal energy like solar ponds, etc. Whereas oceanography, agriculture, astrophysics and various chemical processes also enclosed both thermal and solutal stratification. Furthermore, closed containers, environmental chambers with heated walls are supported by double diffusion occurrence. In fact, stratification plays a dynamic role in many industrial and natural phenomena's.

In practical situations when heat and mass transfer mechanism run simultaneously, it becomes essential to analyse the convective mode of transportation in fluids under the influence of double stratification. The researchers are still busy to explore the characteristics of the mixed convection flows in a doubly stratified frame. Several analytical and experimental attempts have been made for heated surface flows in a stable stratified medium. Yang et al.[1] discussed the laminar free convection flow over a non-isothermal plate embedded in a thermally stratified medium. Transition and stability of buoyancy induced flows in a stratified medium was studied by Jaluria and Gebhart.[2] Thermally stratified fluids flow with natural convection along simple bodies was identified by Chen and Eichhorn.[3] Ishak et al.[4] presented boundary layer fluid flow with dual convection adjacent

[a]Email: taimoor_salahuddin@yahoo.com

to a vertical surface immersed in a stable stratified medium. Chen and Lee[5] considered natural convection effect on micropolar fluid flow along a vertical plate with constant and uniform heat flux in a thermally stratified medium. Singh and Makinde[6] addressed a computational dynamics of magnetohydrodynamic free convection flow over an inclined plate with volumetric heat generation and Newtonian heating. Malik and Rehman[7] reported free convection dissipative fluid flow past over an inclined porous surface by means of heat generation. Mukhopadhyay and Ishak[8] addressed the mixed convection effects over a stretching cylinder in a thermally stratified medium. Singh and Makinde[9] explored the heat transfer characteristics of axisymmetric slip flow by way of vertical cylinder. Hayat et al.[10] studied the stagnation point flow of an Oldroyd-B fluid with thermally stratified medium. Narayana and Murthy[11] presented the free convection effects on power law fluid with heat and mass transfer in a porous doubly stratified medium. Cheng[12] identified free convection flow of power law fluid along a vertical porous wavy surface with collective diffusion of heat and mass as a doubly stratified frame. Double stratified flow of nanofluid over a vertical plate was discussed by Ibrahim and Makinde.[13] Influence of MHD micropolar fluid flow with double stratification was presented by Skrinvasacharya and Upendra.[14] Hayat et al.[15] examined the radiative flow of Jeffrey fluid brought by stretching sheet with double stratification effects. Makinde [16,17] discussed the reactive flow of non-Newtonian fluids in a cylindrical pipe. Furthermore, he reported a thermal analysis of reactive generalized Couette flow regarding power law fluids between concentric cylindrical pipes.

Fluids exhibiting non- Newtonian rheology are still a topic of of great interest because of their concrete applications in metallurgical processes, crystal growth, fiber technology, wire drawing, food products, etc. A single constitutive relationship is not enough to identify the flow characteristics of non-Newtonian fluids. Hence different models of non-Newtonian fluids have been proposed like power law fluid model, Maxwell fluid model, Jeffrey fluid model, Oldroyd-B fluid model, etc. In general, non-Newtonian fluids are classified into three major types namely, differential, rate or integral type. Here, Maxwell fluid is a rate type substance which exhibits just the behavior of relaxtion time. Both relaxtion and retardation characteristics are explained through rate type non-Newtonian fluids like Jeffrey and Oldroyd-B fluids. Whereas, power law model is purely a empirical relation between velocity gradients and stresses. In 1944, owing the importance of non-Newtonian fluid models, Eyring and Powell proposed a distinct fluid model known as Eyring-Powell fluid model (see Ref. 18). Eyring-Powell model has certain advantages over existing non-Newtonian models in this sense that it is obtained from molecular theory of gases rather than the empirical relation. It is important to note that Eyring-Powell fluid turn into Newtonian (viscous) type fluid at high and low shear rates. Even though mathematical structure is complicated but advantages of Eyring-Powell model overcomes its labouring mathematics. Javed et al.[19] investigated the flow of Eyring-Powell fluid brought by stretching sheet. Jalil and Asghar[20] considered the heat and mass transfer effects on Eyring-Powell fluid flow towards a stretching surface. Hayat et al.[21] addressed the stagnation point boundary layer flow of Eyring-Powell fluid with melting heat transfer effect. Khader and Megahed[22] presented numerical findings (utilizing Chebyshev finite difference method) of Eyring-Powell fluid flow induced by time dependent stretching sheet with internal heat generation effect. Eyring-Powell boundary layer fluid flow by way of variable viscosity effect was studied by Malik et al.[23] Heat transfer self-similar solution of Eyring-Powell fluid flow along a moving surface in a parallel free stream was identified by Jalil et al.[24] Ara et al.[25] deliberated the radiation effects on Eyring-Powell boundary layer fluid flow due to exponentially shrinking sheet. Mixed convection effects on an Eyring-Powell fluid flow along a rotating cone was taken by Nadeem and Saleem.[26] Khan et al.[27] studied thermophoretic, heat and mass diffusion in MHD Eyring-Powell fluid flow along a vertical stretching sheet with chemical and joule heating effects. The influence of mixed convection on Eyring-Powell nano fluid flow along a stretching sheet was addressed by Malik et al.[28] Goswami et al.[29] presented the flow of Eyring-Powell fluid in the presence of electroosmosis with interfacial slip effect. Hayat et al.[30] discussed the both numerical and series solution of the Eyring-Powell fluid flow in the presence of internal heat generation/absorption and Newtonian heating effects. The heat transfer along Eyring-Powell fluid flow with variable thermal conductivity was analyzed by Megahed.[31] Panigrahia et al.[32] investigated the mixed convection and thermal diffusion effects on Eyring-Powell fluid flow induced by non-linear stretching surface. Recently, Hayat et al.[33] studied the MHD Eyring-Powell nanofluid flow brought by a stretching cylinder by way of thermal radiation effect.

The above-mentioned literature survey reflects that the investigators restricted their study to horizontal geometry, so the double stratification effects with mixed convection on Eyring-Powell fluid flow carried by an inclined stretching cylinder is not investigated so far. Therefore, current study aims to fill the gap and seems to be a first attempt in this direction to identify the dual stratification effects on Eyring-Powell fluid flow along an inclined stretching cylinder in the presence of mixed convection phenomena and heat generation process. Temperature and concentration are taken as variable quantities at the surface of cylinder and away from it. Numerical solutions are constructed by shooting method. Adopted parameter values for current computational analysis are given as curvature parameter $K = 0.1$, fluid parameters $\lambda = M = 0.1$, mixed convection parameter $\lambda_m = 0.1$, ratio of thermal to concentration buoyancy forces $N = 0.1$, Prandtl number $Pr = 1.3$, thermal stratification parameter $\varepsilon_1 = 0.1$, $\delta_H = 0.1$, Schmidt number $Sc = 0.2$, solutal stratification parameter $\varepsilon_2 = 0.1$ and inclination $\alpha = 30^0$. All graphic results are corresponding to these values unless indicated on appropriate graphs. The influence of different embedded physical parameters on non-dimensional velocity, temperature and concentration profiles are examined graphically. Skin friction-coefficient, local Nusselt and Sherwood numbers are numerically computed against several involved parameters.

II. FLOW ANALYSIS

Consider two dimensional, steady incompressible boundary layer flow of Eyring-Powell fluid over an inclined stretching cylinder. Flow analysis is taken with double stratification in the presence of mixed convection and heat generation/absorption. Temperature as well as concentration at the surface of cylinder is assumed at higher strength than the ambient fluid (see Fig. 1). The rheological equation of state for an incompressible flow of Eyring-Powell fluid is given as:

$$\Gamma = [\ \mu + \frac{1}{\beta\gamma^1}\sinh^{-1}\left(\frac{1}{c}\gamma^1\right)\ \mathbf{A}_1, \tag{1}$$

where

$$\gamma^1 = \sqrt{\frac{1}{2}tr(\mathbf{A}_1)^2}, \tag{2}$$

μ, A_1, tr, β and c are dynamic viscosity, first Rivlin-Ericksen tensor, trace and fluid parameters respectively. For $\sinh^{-1}(\backslash.)$ function, a second order approximation is considered as:

$$\sinh^{-1}(\frac{1}{c}\gamma^1) \cong \frac{\gamma^1}{c} - \frac{{\gamma^1}^3}{6c^3},\ \text{where}\ \left|\frac{1}{c}\gamma^1\right| \ll 1. \tag{3}$$

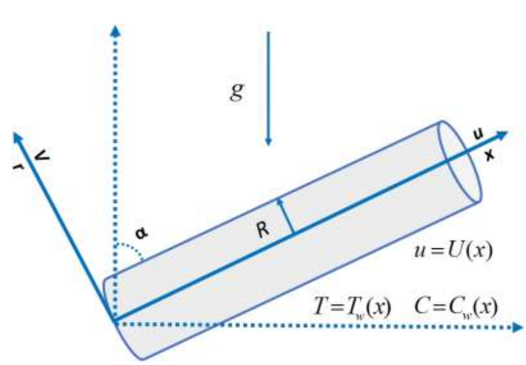

FIG. 1. Physical configuration and coordinate system.

By using the velocity field vector $\mathbf{V} = [v(x,r), 0, u(x,r)]$, the boundary layer approximation reduces the mass conservation and momentum equations to:

$$\frac{\partial (ru)}{\partial x} + \frac{\partial (rv)}{\partial r} = 0, \tag{4}$$

$$u\frac{\partial u}{\partial x} + v\frac{\partial u}{\partial r} = \left(\nu + \frac{1}{\beta \rho c}\right)\frac{\partial^2 u}{\partial r^2} - \frac{1}{2\beta c^3 \rho}\left(\frac{\partial u}{\partial r}\right)^2 \frac{\partial^2 u}{\partial r^2} + \frac{1}{r}\left(\nu + \frac{1}{\beta \rho c}\right)\frac{\partial u}{\partial r} - \frac{1}{6\beta r \rho c^3}\left(\frac{\partial u}{\partial r}\right)^3 + \left(g\beta_T (T - T_\infty) + g\beta_c (C - C_\infty)\right)\cos\alpha. \tag{5}$$

The axial axis of cylinder is supposed as x-axis and r-axis is perpendicular to it. So that, in the above expressions, the velocity components u and v are in the x and r direction respectively. Whereas, ν, $\rho, \sigma, g, \beta_T, \beta_C, \alpha$ denotes kinematic viscosity, fluid density, electrical conductivity, gravity, coefficient of thermal expansion, coefficient of concentration expansion and inclination of cylinder with x-axis respectively. Note that β and c are the the Eyring-Powell fluid parameters. The corresponding boundary conditions of problem are

$$u(x,r) = U(x) = \frac{U_0}{L}x, \quad v(x,r) = 0 \quad \text{at} \quad r = R \quad \text{and} \quad u(x,r) \to 0 \quad \text{as} \quad r \to \infty. \tag{6}$$

Where ψ is the stream function, which identically satisfies the continuity Eq. (4) and is defined as

$$u = \frac{1}{r}\left(\frac{\partial \psi}{\partial r}\right), \quad v = \frac{-1}{r}\left(\frac{\partial \psi}{\partial x}\right). \tag{7}$$

To trace out the solution of Eq. (5) under boundary conditions Eq. (6) we used following transformations:

$$u = \frac{U_0 x}{L} f'(\eta), \; v = -\frac{R}{r}\sqrt{\frac{U_0 \nu}{L}} f(\eta), \; \eta = \frac{r^2 - R^2}{2R}\left(\frac{U_0}{\nu L}\right)^{\frac{1}{2}}, \quad \psi = \left(\frac{U_0 \nu x^2}{L}\right)^{\frac{1}{2}} R f(\eta), \tag{8}$$

where U_0 is the free stream velocity, L is the reference length, $f(\eta)$ represents dimensionless variable and prime denotes differentiation with respect to η (similarity variable) so that, $f'(\eta)$ is the velocity of fluid over an inclined stretching cylinder having radius R. Once incorporating Eqs. (7)-(8) into Eq. (5), we get

$$(1 + 2K\eta)(1 + M) f''' + f f'' - (f')^2 + 2K(1 + M) f'' - \frac{4}{3}\lambda M K (1 + 2K\eta)(f'')^3 - M\lambda (1 + 2K\eta)^2 (f'')^2 f''' + \lambda_m (\theta + N\phi)\cos\alpha = 0, \tag{9}$$

the reduced boundary conditions of problem are given as:

$$f(0) = 0, \; f'(0) = 1 \text{ and } f'(\infty) \to 0. \tag{10}$$

Here K, M, λ, λ_m, and N denotes curvature parameter, fluid parameters, mixed convection parameter and ratio of thermal to concentration buoyancy forces respectively. They are defined as follows:

$$K = \frac{1}{R}\sqrt{\frac{\nu}{a}}, \; M = \frac{1}{\mu\beta c}, \; \lambda = \frac{a^3 x^2}{2c^2 \nu}, \; \lambda_{\mathrm{m}} = \frac{Gr}{\mathrm{Re}_x{}^2}, \; N = \frac{Gr}{Gr^*} \text{ and } a = \frac{U_0}{L}, \tag{11}$$

where Gr and Gr^* denotes Grashof number due to temperature and concentration respectively and defined as:

$$Gr = \frac{g\beta_T (T_w - T_0) x^3}{\nu^2}, \; Gr^* = \frac{g\beta_C (C_w - C_0) x^3}{\nu^2}. \tag{12}$$

The skin friction coefficient at the surface of cylinder is considered as:

$$C_f = \frac{\tau_w}{\rho \frac{U^2}{2}}, \tag{13}$$

$$\tau_w = \left[\mu\left(\frac{\partial u}{\partial r}\right) + \frac{1}{\beta c}\frac{\partial u}{\partial r} - \frac{1}{6\beta c^3}\left(\frac{\partial u}{\partial r}\right)^3\right]_{r=R}, \tag{14}$$

where μ denotes viscosity of fluid and τ_w is the shear stress. The dimensionless form of skin friction coefficient is given by

$$C_f \,\mathrm{Re}_x^{1/2} = 2(1+M)f''(0) - \frac{2M\lambda}{3}(f''(0))^3, \tag{15}$$

with $\mathrm{Re}_x = \frac{U_0 x^2}{\nu L}$ as a local Reynolds number.

III. HEAT AND MASS ANALYSIS

Heat analysis is carried out in the presence of heat generation/absorption. The destruction of fluctuation velocity gradients by action of viscous stresses in a laminar boundary layer flow of Eyring-Powell fluid is assumed to be small, so the viscous dissipation is neglected. Than under boundary layer approximation the energy and concentration equations takes the form:

$$u\frac{\partial T}{\partial x} + v\frac{\partial T}{\partial r} = \frac{\kappa}{\rho \mathrm{c_p}}\frac{\partial}{r\,\partial r}\left(r\frac{\partial T}{\partial r}\right) + \frac{Q_0}{\rho c_p}, \tag{16}$$

$$u\frac{\partial C}{\partial x} + v\frac{\partial C}{\partial r} = D\left(\frac{\partial^2 C}{\partial r^2} + \frac{1}{r}\frac{\partial C}{\partial r}\right), \tag{17}$$

where κ denotes thermal conductivity, c_p is specific heat at constant pressure, D be the mass diffusivity and Q_0 is the heat generation and absorption coefficient. Temperature and concentration boundary conditions for the fluid flow problem are given by

$$\begin{aligned} &T(x,r) = T_w(x) = T_0 + \frac{b\,x}{L}, \quad C(x,r) = C_w(x) = C_0 + \frac{d\,x}{L} \quad \text{at} \quad r = R, \\ &T(x,r) \to T_\infty(x) = T_0 + \frac{c\,x}{L}, \quad C(x,r) \to C_\infty(x) = C_0 + \frac{e\,x}{L} \quad \text{as} \quad r \to \infty, \end{aligned} \tag{18}$$

where $T_w(x)$, $C_w(x)$, $T_\infty(x)$, $C_\infty(x)$, T_0, C_0 denotes prescribed surface temperature, surface concentration, variable ambient temperature, variable ambient concentration, reference temperature and reference concentration respectively, where *b, c, d* and *e* are positive constants. To find out the dimensionless form of Eq. (16) and Eq. (17) under boundary conditions i-e Eq. (18), we considered η, $\theta(\eta)$ and $\phi(\eta)$ defined as:

$$\eta = \frac{r^2 - R^2}{2R}\left(\frac{U_0}{\nu L}\right)^{\frac{1}{2}}, \ \theta(\eta) = \frac{T - T_\infty}{T_w - T_0}, \ \phi(\eta) = \frac{C - C_\infty}{C_w - C_0}, \tag{19}$$

after substituting Eq. (19) in Eqs. (16)-(17), than the dimensionless form of energy and concentration equations are given as:

$$(1+2K\eta)\,\theta'' + 2K\theta' + \mathrm{Pr}\,(f\,\theta' - f'\theta - f'\,\varepsilon_1 + \delta_H\theta) = 0, \tag{20}$$

$$(1+2K\eta)\,\phi'' + 2K\phi' + Sc\,(f\phi' - f'\phi - f'\,\varepsilon_2) = 0, \tag{21}$$

subjected to the transformed boundary conditions:

$$\begin{aligned} &\theta = 1 - \varepsilon_1 \quad \phi = 1 - \varepsilon_2, \quad \text{at} \quad \eta = 0, \\ &\theta \to 0 \quad \phi \to 0, \ \text{as} \quad \eta \to \infty, \end{aligned} \tag{22}$$

where Pr, ε_1, δ_H, Sc and ε_2 denotes Prandtl number, thermal stratification parameter, heat generation/absorption parameter, Schmidt number and solutal stratification parameter respectively and given as follows:

$$\mathrm{Pr} = \frac{\mu c_p}{\kappa}, \quad \varepsilon_1 = \frac{c}{b}, \quad \delta_H = \frac{LQ_0}{U_0\rho c_p}, \quad Sc = \frac{\nu}{D}, \quad \varepsilon_2 = \frac{e}{d}. \tag{23}$$

The local Nusselt and Sherwood numbers are defined as:

$$Nu_x = \frac{xq_w}{k(T_w - T_\infty)}, \quad q_w = -k\left(\frac{\partial T}{\partial r}\right)_{r=R}, \tag{24}$$

$$Sh = \frac{-xj_w}{D(C_w - C_0)}, \quad j_w = -D\left(\frac{\partial C}{\partial r}\right)_{r=R}, \tag{25}$$

in dimensionless form, these quantities can be defined as:

$$Nu_x \mathrm{Re}_x^{-1/2} = -\theta'(0)\,, \tag{26}$$

$$Sh \mathrm{Re}_x^{-1/2} = -\phi'(0)\,. \tag{27}$$

IV. NUMERICAL RESULTS AND DISCUSSION

The system of governing coupled non-linear ordinary differential equations i-e Eqs. (9), (20) and (21) subjected to boundary conditions Eqs. (10) and (22) is solved by employing shooting method with the aid of fifth order Runge-Kutta scheme. Firstly, reduction has been done in a system of seven first order simultaneous equations by letting

$$\begin{aligned} z_2 &= f', \\ z_3 &= z'_3 = f'', \\ z_5 &= \theta', \\ z_7 &= \phi', \end{aligned}$$

than the equivalent form of Eqs. (9), (20) and (21) under new variables is given by:

$$\left[\begin{aligned} &z'_1 = z_2 \\ &z'_2 = z_3 \\ &z'_3 = \frac{(z_2)^2 - z_1 z_3 - (2K)(1+M)z_3 + \frac{4}{3}\lambda MK(1+2K\eta){z_3}^3 - \lambda_T(z_4 + Nz_6)\cos\alpha}{(1+2K\eta)(1+M) - M\lambda(1+2K\eta)^2{z_3}^2} \\ &z'_4 = z_5 \\ &z'_5 = \frac{\Pr(z_2 z_4 + \varepsilon_1 z_2 - z_1 z_5 - \delta_H z_4) - 2Kz_5}{1+2K\eta} \\ &z'_6 = z_7 \\ &z'_7 = \frac{Sc(z_2 z_6 + \varepsilon_2 z_2 - z_1 z_7) - 2Kz_7}{1+2K\eta} \end{aligned}\right], \tag{28}$$

the corresponding boundary conditions in new variables are given as follows:

$$\begin{aligned} z_1(0) &= 0, \\ z_2(0) &= 1, \\ z_3(0) &= unknown, \\ z_4(0) &= 1 - \varepsilon_1, \\ z_5(0) &= unknown, \\ z_6(0) &= 1 - \varepsilon_2, \\ z_7(0) &= unknown. \end{aligned} \tag{29}$$

In order to integrate Eq. (28) as an initial value problem, we required values for $z_3(0)$ i.e. $f''(0)$, $z_5(0)$ i.e. $\theta'(0)$ and $z_7(0)$ implies $\phi'(0)$. The initial conditions $z_3(0)$, $z_5(0)$, $z_7(0)$ are not given but we have additional boundary conditions:

$$\begin{aligned} z_2(\infty) &= 0, \\ z_4(\infty) &= 0, \\ z_6(\infty) &= 0. \end{aligned} \tag{30}$$

TABLE I. Numerical values of skin friction coefficient fo K, Pr and M.

K	Pr	M	$\frac{1}{2}C_f\mathrm{Re}_x^{1/2} = (1+M)f''(0) - \frac{M\lambda}{3}(f''(0))^3$
0.1	1.1	0.1	-0.9809
0.2	-	-	-1.0254
0.3	-	-	-1.0694
0.1	1.1	0.1	-0.9809
-	1.2	-	-0.9825
-	1.3	-	-0.9839
0.1	1.1	0.1	-0.9809
-	-	0.2	-1.0268
-	-	0.3	-1.0779

By choosing favourable guessed values of $f''(0)$, $\theta'(0)$ and $\phi'(0)$, the integration of system of first order differential equations are carried out in a such a way that the boundary conditions given in Eq. (30) holds absolutely. The step size $\Delta\eta = 0.05$ is used to obtain the numerical solution with four decimal accuracy as convergence criteria.

Table I and Table II are constructed to indicate the influence of embedded physical parameters symbolically, K, Pr, M, λ , Sc, ε_1, ε_2 on skin friction coefficient. Adopted parametric values are mixed convection parameter $\lambda_m = 0.1$, ratio of buoyancy forces $N = 0.1$, inclination angle $\alpha = 30^0$ and heat generation/absorption parameter $\delta_H = 0.1$, it is revealed that skin friction coefficient increases (in absolute sense) for higher values of curvature parameter K, thermal stratification parameter ε_1, solutal stratification parameter ε_2, fluid parameter M, Prandtl number Pr and Schmidt number Sc. Whereas, skin friction coefficient shows declined effect on fluid parameters λ.

Tables III-IV shows the influence of different physical parameters over heat and mass transfer rate for fluid parameters $\lambda = 0.1$ and $M = 0.1$, mixed convection parameter $\lambda_m = 0.1$, ratio of buoyancy forces $N = 0.1$, inclination angle $\alpha = 30^0$ and heat generation/absorption parameter $\delta_H = 0.1$. Particularly, Table III shows rate variation of heat transfer against frequent values of curvature parameter K, Prandtl number Pr and thermal stratification parameter ε_1. Whereas, Table IV shows rate variation of mass transfer rate for different values of curvature parameter K, Schmidt number Sc and solutal stratification parameter ε_2. It is examined that the heat and mass transfer rate increases for larger values of curvature parameter K, Prandtl number Pr and Schmidt number Sc, respectively. Whereas, heat and mass transfer rate exhibits decreasing behavior towards thermal stratification parameter ε_1 and solutal stratification parameter ε_2 respectively. By incorporating $M = 0$, $\lambda = 0$, $\lambda_m = 0$, $\alpha = 0^0$, $\varepsilon_1 = 0$ and $\delta_{\mathrm{H}} = 0$, eq. (9) and eq. (20) reduces to the flow problem identified by Ishak and Nazar.[29] Furthermore, in the absence of curvature parameter (i-e K= 0) with

TABLE II. Numerical values of skin friction coefficient for λ, Sc, ε_1 and ε_2.

λ	Sc	ε_1	ε_2	$\frac{1}{2}C_f\mathrm{Re}_x^{1/2} = (1+M)f''(0) - \frac{M\lambda}{3}(f''(0))^3$
0.1	0.2	0.1	0.1	-0.9809
0.2	-	-	-	-0.9760
0.3	-	-	-	-0.9738
0.1	0.2	0.1	0.1	-0.9809
-	0.3	-	-	-0.9850
-	0.4	-	-	-0.9893
0.1	0.2	0.1	0.1	-0.9809
-	-	0.2	-	-0.9868
-	-	0.3	-	-0.9937
0.1	0.2	0.1	0.1	-0.9809
-	-	-	0.2	-0.9887
-	-	-	0.3	-0.9995

TABLE III. Temperature gradient at the outer surface of cylinder for various values of K, Pr and ε_1.

K	Pr	ε_1	$-\theta'(0)$
0.1	1.1	0.1	1.0983
0.2	-	-	1.1306
0.3	-	-	1.1632
0.1	1.1	0.1	1.0983
-	1.2	-	1.1553
-	1.3	-	1.2101
0.1	1.1	0.1	1.0983
-	-	0.2	1.0567
-	-	0.3	1.0144

$M = 0$, $\lambda = 0$, $\lambda_m = 0$, $\alpha = 0^0$, $\varepsilon_1 = 0$ and $\delta_H = 0$, eq. (9) and eq. (20) reduces to the flow problem given by Grubka and Bobba.[30] Table V is constructed to compare the heat transfer rate for various values of Prandtl number Pr in a limited sense. An excellent agreement has been found which leads to conformity of present work.

A. Velocity Profiles

Figs. 2-8 illustrate the effects of flow controlling parameters over non-dimensional velocity profiles. Fig. 2 shows that an increase in thermal stratification parameter ε_1 leads to decrease in velocity profile. This effect is due to drop of convective potential between surface of cylinder and ambient temperature. Fig. 3 identify that an increase in mixed convection parameter λ_m brings increase in fluid velocity. Physically, this is due to enhancement of thermal buoyancy force. So higher values of mixed convection parameter λ_m leads to increase in velocity within a boundary layer. The behaviour of an inclination α over velocity is depicted in Fig. 4. It is noticed that for higher values of an inclination α the velocity profile declines. Because by increasing an inclination α relative to x-axis the influence of gravity is reduced which results decline in velocity within a boundary layer. Fig. 5 illustrates that for larger values of curvature parameter K the radius of cylinder decreases and fluids motion accelerates. This is due to reduction of contact surface area of cylinder with fluid which offers less resistance to fluid flow. So increase in curvature parameter K cause increase in velocity profile within the boundary layer. The effect of solutal stratification parameter ε_2 over velocity is displayed in Fig. 6. It is observed that the fluid velocity decreases within boundary layer for the increasing values of solutal stratification parameter ε_2. Fig. 7 is the evident that the velocity profile increases against increasing value of fluid parameter M. Because fluid parameter M has inverse relation with viscosity so higher values of fluid parameter M brings fluid to be less viscous which results increased in rate of deformation. Fig. 8 is sketched to examine the effects of ratio of buoyancy forces N on velocity profile. As N is the ratio of concentration to the

TABLE IV. Mass transfer rate at outer surface of cylinder for different values of K, Sc and ε_2.

K	Sc	ε_2	$-\phi'(0)$
0.1	0.2	0.1	0.4500
0.2	-	-	0.5020
0.3	-	-	0.5512
0.1	0.2	0.1	0.4500
-	0.3	-	0.5220
-	0.4	-	0.6068
0.1	0.2	0.1	0.4500
-	-	0.2	0.4013
-	-	0.3	0.3711

TABLE V. Comparison of heat transfer rate for different value of Prandtl number Pr.

Pr	Grubka and Bobba [35]	Ishak and Nazar [34]	Present study
0.72	*0.8086*	*0.8086313*	*0.8089*
1.00	*1.000*	*1.0000000*	*1.0000*
3.00	*1.9237*	*1.9236825*	*1.9239*
10.0	*3.7207*	*3.7206739*	*3.7208*

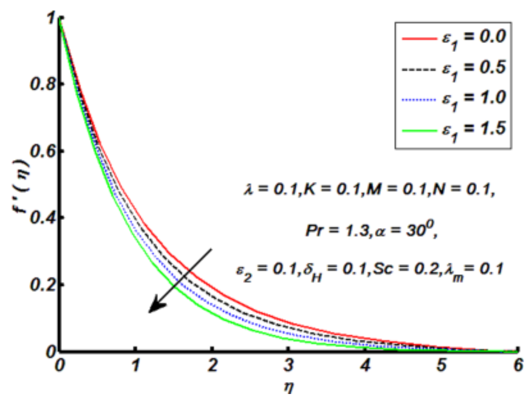

FIG. 2. Effect of thermal stratification parameter ε_1 over velocity profile.

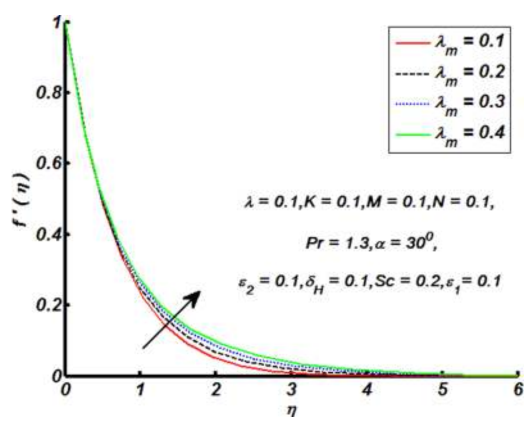

FIG. 3. Effect of mixed convection parameter λ_m over velocity profile.

thermal buoyancy forces, so larger values of buoyancy forces N reflects dominancy in concentration buoyancy force which yields increased in velocity distribution within a boundary layer.

B. Temperature Profiles

Figs. 9-14 reflect the impacts of different physical flow parameters over temperature profiles. Influence of thermal stratification parameter ε_1 over temperature profile is given by Fig. 9. It is prominent from figure that the temperature distribution decreases for increasing values of thermal stratification parameter ε_1. This outcome is due to declined in temperature difference between surface of cylinder and ambient fluid, hence temperature profile decreases within thermal boundary layer. Fig. 10 provides the influence of an inclination α against temperature distribution. It is noticed that increase in an inclination α produces enhancement in temperature within a boundary layer. This fact is due to fall down of gravity effect. For larger values of an inclination α the gravity effect reduces which results decrease in rate of heat transfer. Therefore temperature distribution

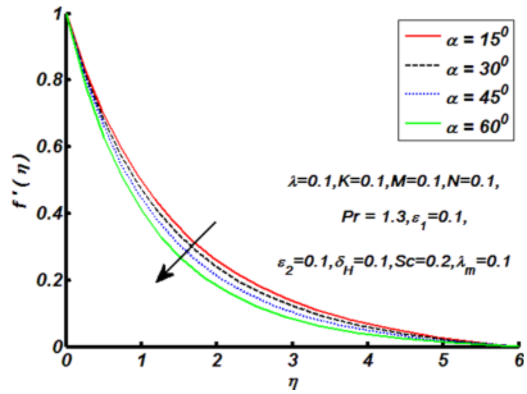

FIG. 4. Effect of an inclination α over velocity profile.

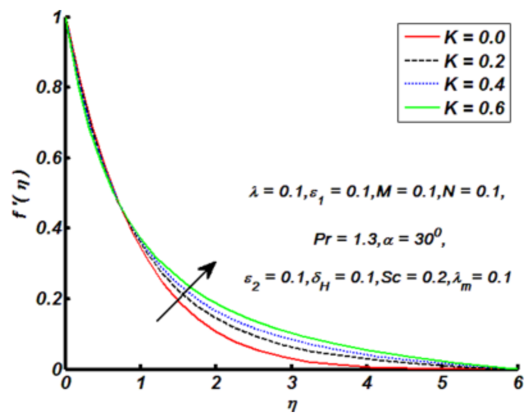

FIG. 5. Effect of curvature parameter K over velocity profile.

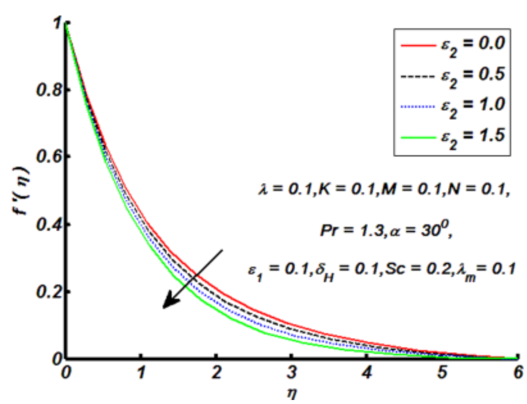

FIG. 6. Effect of solutal stratification parameter ε_2 over velocity profile.

increases. Fig. 11 elaborates the influence of heat generation/heat absorption parameter δ_H over temperature distribution. It is explored that increase in heat generation/heat absorption parameter δ_H causes increase in temperature of fluid. Here significant heat is produced during heat generation phenomena which results increase in temperature distribution. Fig. 12 illustrates that the temperature distribution increases due to increase in curvature parameter K. Kelvin temperature is state as an average kinetic energy so, when we increase curvature parameter K of cylinder, velocity of the fluid increases which results increase in kinetic energy and due to which temperature increases. Note that temperature profile decreases adjacent to the surface of cylinder and increases away from

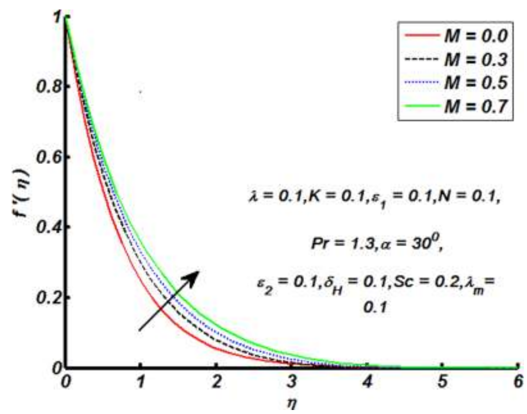

FIG. 7. Effect of fluid parameter M over velocity profile.

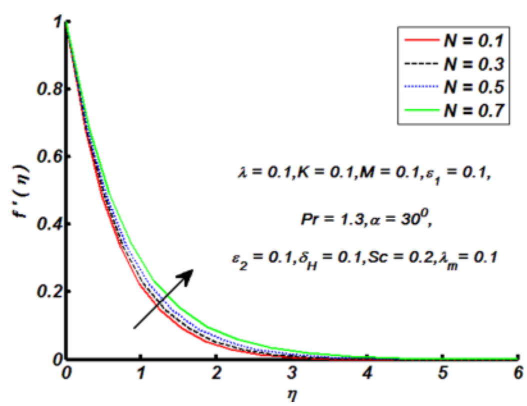

FIG. 8. Effect of ratio of buoyancy forces N over velocity profile.

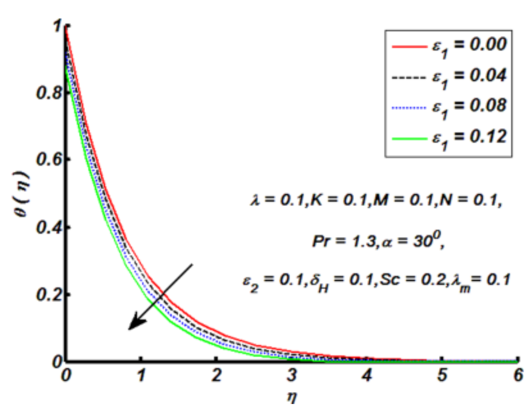

FIG. 9. Effect of thermal stratification parameter ε_1 over temperature profile.

it. It is clearly seen that an increase in intensity of buoyancy forces marks increase in temperature of fluid. Fig. 13 is the evident that the temperature distribution increases for higher values of solutal stratification parameter ε_2. Fig. 14 presents the influence of Prandtl number Pr on temperature profile. Prandtl number Pr has inverse relation towards thermal conductivity, fluid with higher Prandtl number Pr possesses weak energy diffusion. So, an increase in Prandtl number Pr causes a strong reduction in temperature of the fluid which results thinner thermal boundary layer. Sometimes we may have overshoot in the thermal boundary layer due to higher thermal conductivity. That effect can be controlled by introducing heat sink which helps to moderate the temperature.

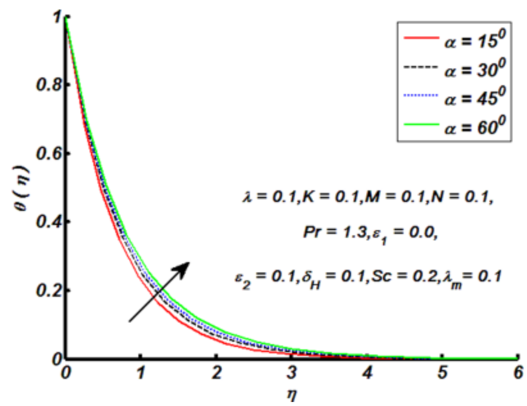

FIG. 10. Effect of an inclination α over temperature profile.

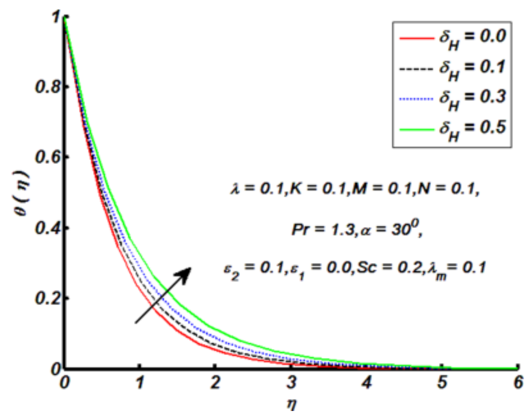

FIG. 11. Effect of heat generation/absorption parameter δ_H over temperature profile.

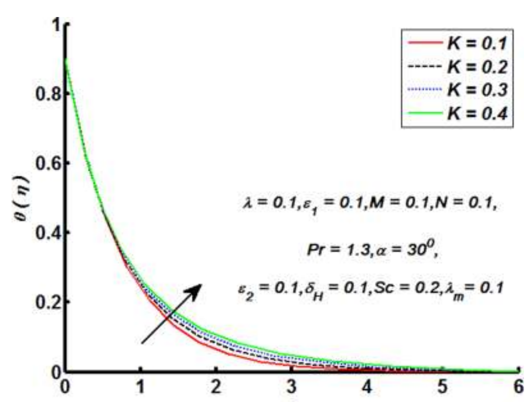

FIG. 12. Effect of curvature parameter K over temperature profile.

C. Concentration profiles

Figs. 15-20 include the effects of several involved parameters over concentration profiles and dimensionless quantities. Fig. 15 demonstrates the impact of thermal stratification parameter ε_1 on concentration profile. An increase in thermal parameter ε_1 brings inciting in fluid concentration across the surface of cylinder. From Fig. 16, it is witnessed that the concentration boundary layer decreases by increasing Schmidt number Sc. Since this effect is similar to Pr verses thermal boundary layer. As Sc has inverse proportional attitude towards mass diffusivity so higher values of

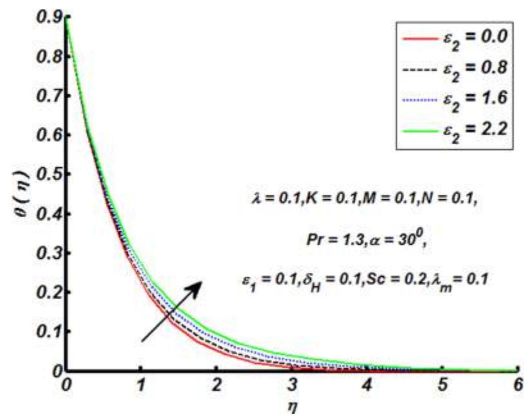

FIG. 13. Effect of solutal stratification parameter ε_2 over temperature profile.

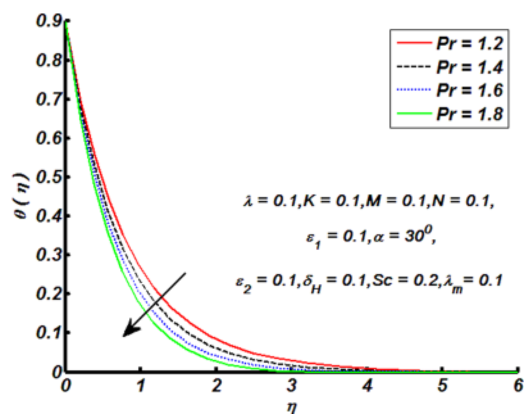

FIG. 14. Effect of Prandtl number Pr over temperature profile.

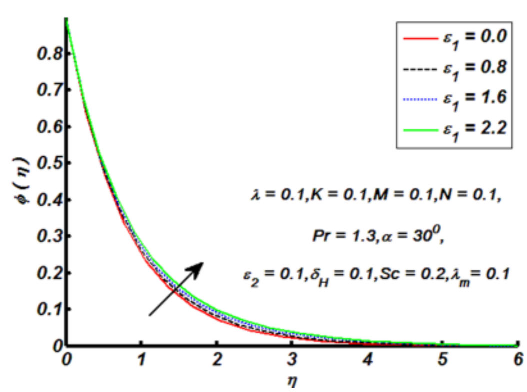

FIG. 15. Effect of thermal stratification parameter ε_1 over concentration profile.

Schmidt number Sc brings thinning in the concentration boundary layer as a result concentration distribution decreases. Influence of solutal stratification parameter ε_2 is described through Fig. 17 over concentration profile. It is clear that concentration boundary layer thickness decreases for higher values of solutal stratification coefficient ε_2. Influence of an inclination α and mixed convection parameter λ_m over skin friction coefficient for both plate and cylinder is sketched in Fig. 18. It is acknowledged that for increasing values of an inclination α skin friction coefficient increases whereas it shows opposite attitude for mixed convection parameter λ_m. Further, the magnitude of skin friction coefficient is higher for cylinder as compare to plate (in absolute sense). Fig. 19 is

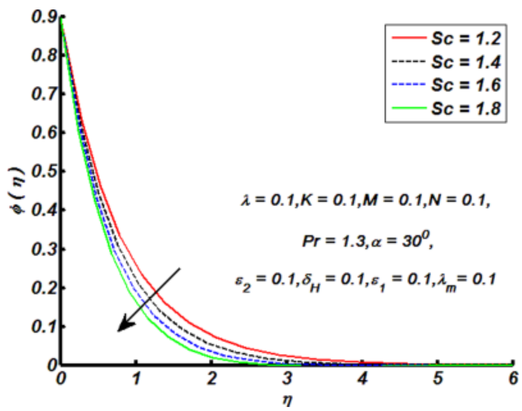

FIG. 16. Effect of Schmidt number Sc over concentration profile.

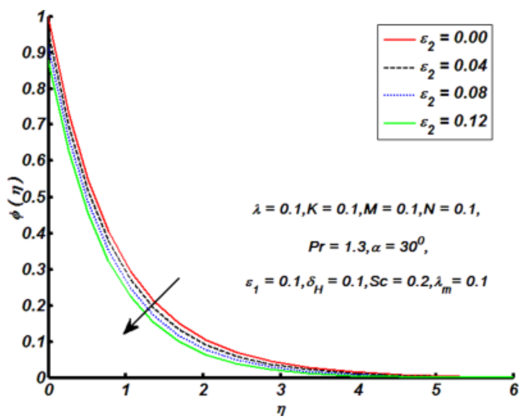

FIG. 17. Effect of solutal stratification parameter ε_2 over concentration profile.

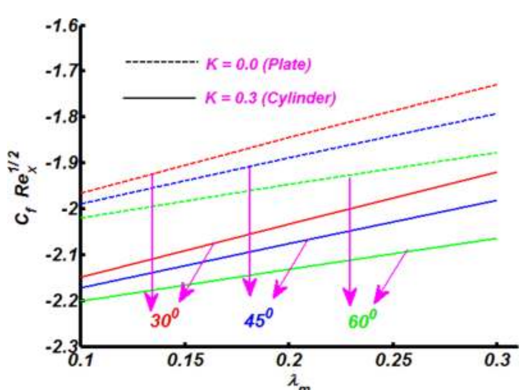

FIG. 18. Effect of an inclination α and mixed convection λ_m over skin friction.

the evident that mass transfer rate decreases for larger values of an inclination α and heat generation/absorption parameter δ_H. It is also absorbed that the strength of mass transfer rate is slightly larger for cylinder with respect to plate. Fig. 20 is constructed to examine the behaviour of mixed convection λ_m and ratio of thermal to concentration buoyancy forces N over mass transfer rate. It is analysed that for greater values of both mixed convection parameter λ_m and ratio of buoyancy forces N the mass transfer rate increases. The magnitude of mass transfer rate significantly incited for cylinder as compare to plate.

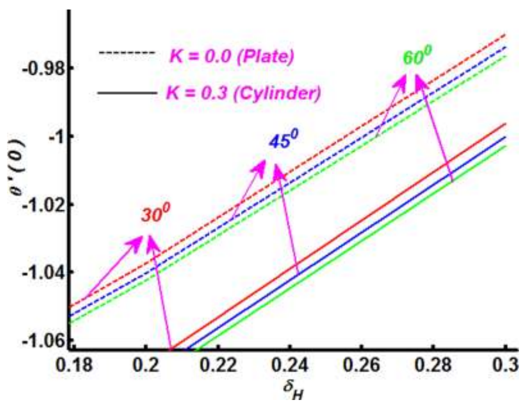

FIG. 19. Effect of an inclination α and heat generation parameter δ_H on local Nusselt number.

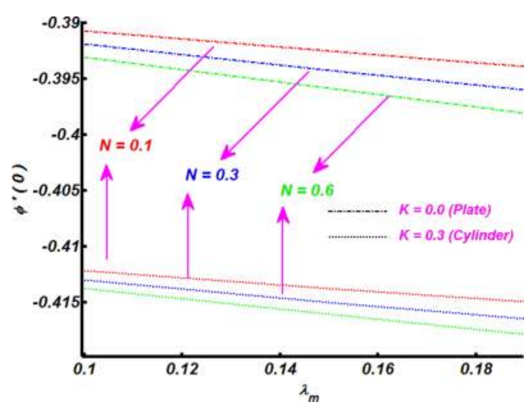

FIG. 20. Effect of mixed convection λ_m and ratio of buoyancy forces N over local Sherwood number.

V. CONCLUSION

Double stratified mixed convection boundary layer flow of Eyring-Powell fluid induced by an inclined stretching cylinder is reported. Flow analysis is carried out with heat generation process. The characteristics of dimensionless velocity, temperature and concentration profiles are acknowledged under the influence of involved flow controlling physical parameters. Dimensionless variables are computed numerically and analysed through graphs for both plate and cylindrical geometry. The summarized findings of present study are listed as follows:

- The fluid velocity increases significantly for larger values of curvature parameter K, fluid parameter M, mixed convection parameter λ_m and ratio of buoyancy forces N. Whereas, velocity profile shows opposite attitude towards thermal stratification parameter ε_1, solutal stratification parameter ε_2 and an inclination α.
- The fluid temperature is increasing function of solutal stratification parameter ε_2, curvature parameter K, an inclination α and heat generation/absorption parameter δ_H. Whereas, its shows decline for thermal stratification parameter ε_1 and Prandtl number Pr.
- The concentration profile increases for increasing values of thermal stratification parameter ε_1 while it decreases for solutal stratification parameter ε_2 and Schmidt number Sc.
- Skin friction coefficient expressively enriches for cylinder as compare to plate regarding an inclination α and reduces for mixed convection parameter λ_m.
- Higher values of an inclination α and heat generation/absorption parameter δ_H shows reduction in heat transfer rate.
- Mass transfer rate considerably increases for both mixed convection parameter λ_m and ratio of buoyancy forces N.

- A comparison between previously published literature Ref. 34 and 35 for heat transfer rate against different values of Prandtl number *Pr* leads to conformity of the present work.

[1] K.T. Yang, J.L. Novotny, and Y.S. Cheng, "Laminar free convection from a non-isothermal plate immersed in a temperature stratified medium," International Journal of Heat and Mass Transfer **15**, 1097-1109 (1972).
[2] Y. Jaluria and B. Gebhart, "Stability and transition of buoyancy-induced flows in a stratified medium," Journal of Fluid Mechanics **66**, 593-612 (1974).
[3] C.C. Chen and R. Eichhorn, "Natural convection from simple bodies immersed in thermally stratified fluids," The ASME Journal of Heat Transfer **98**, 446-451 (1976).
[4] A. Ishak, R. Nazar, and I. Pop, "Mixed convection boundary layer flow adjacent to a vertical surface embedded in a stable stratified medium," International Journal of Heat and Mass Transfer **51**, 3693-3695 (2008).
[5] CL. Chang and ZY. Lee, "Free convection on a vertical plate with uniform and constant heat flux in a thermally stratified micropolar fluid," Mechanics Research Communications **35**, 421–427 (2008).
[6] G. Singh and O.D. Makinde, "Computational dynamics of MHD free convection flow along an inclined plate with Newtonian heating in the presence of volumetric heat generation," Chemical Engineering Communications **199**, 1144-1154 (2012).
[7] M.Y. Malik and Khalil Ur Rehman, "Effects of second order chemical reaction on MHD free convection dissipative fluid flow past an inclined porous surface by way of heat generation: A Lie group analysis," Information Sciences Letters **5**, 35-45 (2016).
[8] S. Mukhopadhyay and A. Ishak, "Mixed convection flow along a stretching cylinder in a thermally stratified medium," Journal of Applied Mathematics doi: (2012).
[9] G. Singh and O.D. Makinde, "Axisymmetric slip flow on a vertical cylinder with heat transfer," Sains Malaysiana **43**, 483-489 (2014).
[10] T. Hayat, Z. Hussain, M. Farooq, A. Alsaedi, and M. Obaid, "Thermally stratified stagnation point flow of an Oldroyd-B fluid," International Journal of Non-Linear Science and Numerical Simulation **15**, 77-86 (2014).
[11] P.A Lakshmi Narayana and P.V.S.N. Murthy, "Free convective heat and mass transfer in a doubly stratified porous medium saturated with a power law fluid," International Journal of Fluid Mechanics Research **36**, 524-537 (2007).
[12] C.Y. Cheng, "Combined heat and mass transfer in natural convection flow from a vertical wavy surface in a power-law fluid saturated porous medium with thermal and mass stratification," International Communications in Heat and Mass **36**, 351-356 (2009).
[13] W. Ibrahim and O.D. Makinde, "The effect of double stratification on boundary layer flow and heat transfer of nanofluid over a vertical plate," Computers and Fluids **86**, 433-441 (2013).
[14] D. Srinivasacharya and M. Upendar, "Effect of double stratification on MHD free covection in a micropolar fluid," Journal of the Egyptian Mathematical Society **21**, 370-378 (2013).
[15] T. Hayat, T. Hussain, S.A Shehzad, and A. Alsaedi, "Thermal and concentration stratifications effects in raditaive flow of Jeffrey fluid over a stretching sheet," Plos one **9**, 1-15 (2014).
[16] O.D. Makinde, "Analysis of Non-Newtonian reactive flow in a cylindrical pipe," ASME - Journal of Applied Mechanics **76**, 034502 (2009) 1-5.
[17] O.D. Makinde, "Thermal analysis of a reactive generalized Couette flow of power law fluids between concentric cylindrical pipes," European Physical Journal Plus **129**, 1-9 (2014).
[18] R.E. Powell and H. Eyring, "Mechanisms for the relaxation theory of viscosity," Nature **154**, 427-428 (1944).
[19] T. Javed, N. Ali, Z. Abbas, and M. Sajid, "Flow of an Eyring- Powell non-Newtonian fluid over a stretching sheet," Chemical Engineering Communications **200**, 327–336 (2013).
[20] M. Jalil and S. Asghar, "Flow and heat transfer of Powell Eyring fluid over a stretching surface: A Lie group analysis," Journal of Fluids Engineering ASME **135**, 121201 (2013).
[21] T. Hayat, M. Farooq, A. Alsaedi, and Z. Iqbal, "Melting heat transfer in the stagnation point flow of Powell Eyring fluid," Journal of Thermophysics and Heat Transfer **27**, 761–766 (2013).
[22] M.M. Khader and M.A. Megahed, "Numerical studies for flow and heat transfer of the Powell-Eyring fluid thin film over an unsteady stretching sheet with internal heat generation using the Chebyshev finite difference method," Journal of Applied Mechanics and Technical Physics **54**, 440–450 (2013).
[23] M.Y. Malik, A. Hussain, and S. Nadeem, "Boundary layer flow of an Eyring-Powell model fluid due to a stretching cylinder with variable viscosity," Scientia Iranica Transactions B: Mechanical Engineering **20**, 313-321 (2013).
[24] M. Jalil, S. Asghar, and S.M. Imran, "Self-similar solutions for the flow and heat transfer of Powell-Eyring fluid over a moving surface in a parallel free stream," International Journal of Heat and Mass Transfer **65**, 73-79 (2013).
[25] A. Ara, N.A. Khan, H. Khan, and F. Sultan, "Radiation effect on boundary layer flow of an Eyring-Powell fluid over an exponentially shrinking sheet," Ain-Shams Engineering Journal **5**, 1337-1342 (2014).
[26] S. Nadeem and S. Saleem, "Mixed convection flow of Eyring–Powell fluid along a rotating cone," Results in Physics **4**, 54–62 (2014).
[27] N.A. Khan, F. Sultan, and Nadeem A. Khan, "Heat and mass transfer of thermophoretic MHD flow of Powell-Eyring fluid over a vertical stretching sheet in the presence of chemical reaction and Joule heating," International Journal of Chemical Reactor Engineering DOI:.
[28] M.Y. Malik, I. Khan, A. Hussain, and T. Salahuddin, "Mixed convection flow of MHD Eyring-Powell nanofluid over a stretching sheet: A numerical study," AIP Advances **5**, 117118, doi: (2015).
[29] P. Goswami, P.K. Mondal, S. Dutta, and S. Chakraborty, "Electroosmosis of Powell–Eyring fluids under interfacial slip," Electrophoresis **36**, 703–711 (2015).
[30] T. Hayat, S. Ali, M.A. Farooq, and A. Alsaedi, "On comparison of series and numerical solutions for flow of Eyring-Powell fluid with Newtonian heating and internal heat generation/absorption," PLoS One **10**, 1-13 (2015).

[31] M.A. Megahed, “Flow and heat transfer of Powell-Eyring fluid due to an exponential stretching sheet with heat flux and variable thermal conductivity,” Zeitschrift für Naturforschung A **70**, 163-169 (2015).
[32] S. Panigrahia, M. Rezab, and A.K. Mishraa, “Mixed convective flow of a Powell-Eyring fluid over a non-linear stretching surface with thermal diffusion and diffusion thermo,” Procedia Engineering **127**, 645–651 (2015).
[33] T. Hayat, N. Gull, M. Farooq, and B. Ahmad, “Thermal radiation effect in MHD flow of Powell-Eyring nanofluid induced by a stretching cylinder,” Journal of Aerospace Engineering **29**, Doi: (2015).
[34] A. Ishak and R. Nazar, “Laminar boundary flow along a stretching cylinder,” European Journal of Scientific Research **36**, 22-29 (2009).
[35] L.G. Grubka and K.M. Bobba, “Heat transfer characteristics of a continuous stretching surface with variable temperature,” Journal of Heat Transfer **107**, 248-250 (1985).